

New constraints on Planck-scale Lorentz Violation in QED from the Crab Nebula

Luca Maccione^{1,2}, Stefano Liberati^{1,2}, Annalisa Celotti^{1,2}, John G. Kirk³

¹ SISSA, Via Beirut, 2-4, I-34014, Trieste, Italy

² INFN, Sezione di Trieste, Via Valerio, 2, I-34127, Trieste, Italy

³ Max-Planck-Institut für Kernphysik, Saupfercheckweg, 1, D-69117, Heidelberg, Germany

E-mail: maccione@sissa.it, liberati@sissa.it, celotti@sissa.it, John.Kirk@mpi-hd.mpg.de

Abstract. We set constraints on $O(E/M)$ Lorentz Violation in QED in an effective field theory framework. A major consequence of such assumptions is the modification of the dispersion relations for electrons/positrons and photons, which in turn can affect the electromagnetic output of astrophysical objects. We compare the information provided by multiwavelength observations with a full and self-consistent computation of the broad-band spectrum of the Crab Nebula. We cast constraints of order 10^{-5} at 95% confidence level on the lepton Lorentz Violation parameters.

1. Introduction

Local Lorentz Invariance (LI) is fundamental to both of the two pillars of our present physical knowledge: the standard model of particle physics and general relativity. Nonetheless, the most recent progress in theoretical physics, in particular towards the construction of a theory of Quantum Gravity (QG), has led to a new perspective, in which both of the above mentioned theories are seen as effective ones to be replaced by a theory of some more fundamental objects at high energies. From this perspective it is conceivable that even fundamental spacetime symmetries (such as local LI) could cease to be valid in the vicinity of the Planckian regime.

This insight and several other arguments (see, e.g., the discussion in [1, 2, 3, 4]) that question LI at high energies, have been strengthened by specific hints of Lorentz Violation (LV) arising from preliminary calculations in various approaches to QG. Examples include string theory tensor VEVs [5], spacetime foam [6], semiclassical spin-network calculations in Loop QG [7], non-commutative geometry [8, 9, 10], some brane-world backgrounds [11] and condensed matter analogues of “emergent gravity” [12]. Although none of these calculations proves that Lorentz symmetry breaking is a necessary feature of QG, they do stimulate research aimed at understanding the possible measurable consequences of LV.

In recent years, attempts to place constraints on high-energy deviations from LI have mainly focused on modified dispersion relations for elementary particles. In fact, in most of the above mentioned QG models, LV enters through dispersion relations which can be cast in the general form (it is assumed, for simplicity, that rotational invariance is preserved and only boost invariance is affected by Planck-scale corrections):

$$E^2 = p^2 + m^2 + f(E, p; \mu; M) , \quad (1)$$

where we set the low energy speed of light $c = 1$, E and p are the particle energy and momentum, μ is a particle-physics mass-scale (possibly associated with a symmetry breaking/emergence scale) and M denotes the relevant QG scale. Generally, it is assumed that M is of order the Planck mass: $M \sim M_{\text{Pl}} \approx 1.22 \times 10^{19}$ GeV, corresponding to a quantum (or emergent) gravity effect. The function $f(E, p; \mu; M)$ can be expanded in powers of the momentum (energy and momentum are basically indistinguishable at high energies, although they are both taken to be smaller than the Planck scale), and the lowest order LV terms (p^2 and p^3) have been mainly considered [1].

At first sight, it appears hopeless to search for effects suppressed by the Planck scale. Even the most energetic particles ever detected (Ultra High Energy Cosmic Rays, see, e.g., [13, 14]) have $E \lesssim 10^{11}$ GeV $\sim 10^{-8} M_{\text{Pl}}$. However, as discussed below, even tiny corrections can be magnified into a significant effect when dealing with high energies (but still well below the Planck scale), long distances of signal propagation, or peculiar reactions (see, e.g., [1]).

However, it must be stressed that most of the above cited effects require a theoretical framework within which it is possible to justify the use of modified dispersion relations of the form (1), in order to calculate reaction rates and, more generally, to describe fully the particle dynamics.

In this regard, two alternative approaches have been proposed. On the one hand, one can interpret the dispersion relation (1) as a by-product of an Effective Field Theory characterised by Planck suppressed LV operators. On the other hand, such a dispersion relation can be interpreted as the Casimir invariant of some new relativity group (which would then incorporates two invariant scales, c and M_{Pl}). The latter approach goes under the name of “doubly (or deformed)-special relativity” (DSR) [15, 16]. While at the moment there are formulations in momentum space of this proposal, its formulation in coordinate space is still far from being complete as well as an effective quantum field theory implementation of this framework (if any, see e.g. [17]). Lacking such an information about the dynamics implied by the theory it is nowadays very difficult to cast stringent constraints on the DSR framework, in particular the constraint that will be discussed in this work will not apply.

In this paper, we aim instead to improve the constraints obtained in the best studied framework of Effective Field Theory with non-renormalisable (i.e., mass dimension 5 and higher) LV operators (see [1, 18] and references therein). To this end, we compute, within our test theory, the broad band emission of the Crab Nebula (CN), exploiting recent observational and theoretical improvements in our astrophysical knowledge of

this object.

The outline of the paper is the following: in the next section we present our theoretical framework. In Section 3 the current status of the constraints on this test theory is reviewed, briefly describing the main processes involved and the role played so far by the CN. In Section 4 we discuss the current observations of the CN and their theoretical interpretation. Section 5 studies the foreseeable role of the departures from LI in our theory and the processes which are included in the reconstruction of the CN spectrum (from radio to γ -rays). Finally, in Section 6, we discuss the constraints that observations place on the theory and the possible improvements expected from future experiments like GLAST [19].

2. QED with Lorentz Violations at order $O(E/M)$

Myers & Pospelov [18] found that there are essentially only three operators of dimension five, quadratic in the fields, that can be added to the QED Lagrangian preserving rotation and gauge invariance, but breaking local LI † . These terms, which result in a contribution of $O(E/M)$ to the dispersion relation of the particles, are the following:

$$-\frac{\xi}{2M}u^m F_{ma}(u \cdot \partial)(u_n \tilde{F}^{na}) + \frac{1}{2M}u^m \bar{\psi} \gamma_m (\zeta_1 + \zeta_2 \gamma_5)(u \cdot \partial)^2 \psi, \quad (2)$$

where \tilde{F} is the dual of F and $\xi, \zeta_{1,2}$ are dimensionless parameters. All these terms also violate the CPT symmetry (note that while CPT violation implies LV the converse is not true [21]).

From (2) the dispersion relations of the fields are modified as follows. For the photon

$$\omega_\pm^2 = k^2 \pm \frac{\xi}{M} k^3, \quad (3)$$

(the + and − signs denote right and left circular polarisation), while for the fermion (with the + and − signs now denoting positive and negative helicity states)

$$E_\pm^2 = p^2 + m^2 + \eta_\pm \frac{p^3}{M}, \quad (4)$$

with $\eta_\pm = 2(\zeta_1 \pm \zeta_2)$. For the antifermion, it can be shown by simple “hole interpretation” arguments that the same dispersion relation holds, with $\eta_\pm^{af} = -\eta_\mp^f$ where af and f superscripts denote respectively anti-fermion and fermion coefficients [2, 22].

The modified dispersion relations affect standard processes (such as threshold reactions) and permit new processes. Of course, this new physics will be visible only at sufficiently high energies, given that Planck suppression characterises the new relations. To estimate the energy scale, consider, for example, a threshold reaction involving photons and electrons such as photon-photon annihilation, leading to electron-positron pair creation. In such a case the characteristic energy scale of the process – to which

† Actually these criteria allow the addition of other (even CPT) terms, but these would not lead to modified dispersion relations (they can be thought as extra interaction terms) [20].

the LV term $\xi k^3/M$ should be comparable – is the electron mass m_e . Assuming a LV coefficient $O(1)$ the effect of the LV should become visible around the critical energy $k_{\text{cr}} \approx 10$ TeV. While prohibitive for laboratory experiments, this energy is within the range of the observed phenomena in high energy astrophysics.

Observations involving energies of the order of 10 TeV can thus potentially cast an $O(1)$ constraint on the coefficients defined above. But what is the theoretically expected value of the LV coefficients in the dispersion relations (3, 4)? In particular, renormalisation group effects could, in principle, strongly suppress the low-energy values of the LV coefficients even if they are $O(1)$ at high energies. Let us, therefore, consider the evolution of the LV parameters.

Bolokhov & Pospelov [20] recently addressed the problem of calculating the renormalisation group equations for QED and the Standard Model extended with dimension-five operators that violate Lorentz Symmetry. For the case of QED, an approach similar to that of Myers & Pospelov [18] was taken. In this context, the evolution equations for the LV terms in Eq. (2) that produce modifications in the dispersion relations, can be inferred to be

$$\frac{d\zeta_1}{dt} = \frac{25}{12} \frac{\alpha}{\pi} \zeta_1, \quad \frac{d\zeta_2}{dt} = \frac{25}{12} \frac{\alpha}{\pi} \zeta_2 - \frac{5}{12} \frac{\alpha}{\pi} \xi, \quad \frac{d\xi}{dt} = \frac{1}{12} \frac{\alpha}{\pi} \zeta_2 - \frac{2}{3} \frac{\alpha}{\pi} \xi, \quad (5)$$

where $\alpha = e^2/4\pi \simeq 1/137$ ($\hbar = 1$) is the fine structure constant and $t = \ln(\mu^2/\mu_0^2)$ with μ and μ_0 two given energy scales. (Note that the above formulae are given to lowest order in powers of the electric charge, which allows one to neglect the running of the fine structure constant.)

These equations show that the running is only logarithmic and therefore low energy constraints are robust. Moreover, they also show that η_+ and η_- cannot, in general, be equal at all scales.

3. Previous astrophysical constraints on QED with $O(E/M)$ LV

Having addressed the issue of the natural values expected for the LV coefficients, we summarise here the current status of the astrophysical constraints on our test theory (see figure 1) and briefly explain how these constraints are obtained.

3.1. Photon time of flight

Although these kinds of constraint are not directly relevant to our work, and currently provide limits several orders of magnitude weaker than those we shall present, we briefly discuss them, because they are widely considered in the astrophysical community.

The dispersion relation (3) implies that photons of different colours (wave vectors k_1 and k_2) travel at slightly different speeds. When accumulated over a cosmological distance d , this effect produces a time delay

$$\Delta t = \xi(k_2 - k_1)d/M, \quad (6)$$

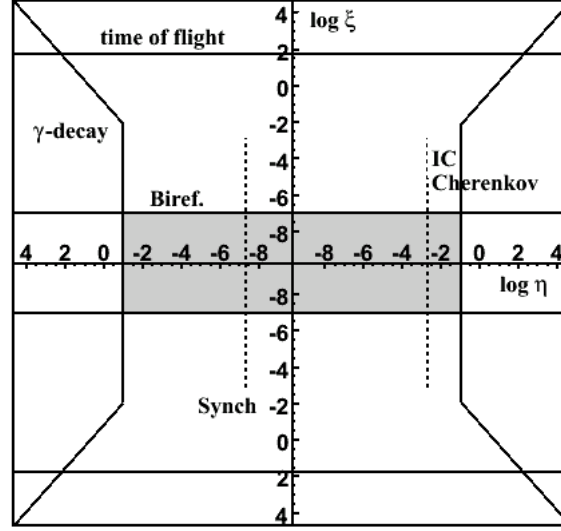


Figure 1. Present constraints on the LV coefficients for QED with dimension 5 Lorentz violation. The grey area is the allowed one and, within it, the region bounded by the two dashed vertical lines identifies the allowed range for at least one of the four lepton LV coefficients (if one assumes that a single lepton population is responsible for the synchrotron and inverse Compton emission of the CN simultaneously).

which clearly increases with d and with the energy difference. The largest systematic error affecting this method is the uncertainty about whether photons of different energy are produced simultaneously in the source (e.g., a Gamma-Ray Burst, GRB). One way of avoiding this problem, available only in the context of our test theory, would be to measure the velocity difference of the two polarisation states at a single energy, corresponding to

$$\Delta t = 2|\xi|k d/M. \quad (7)$$

However, this bound would require that both polarisations are observed and that no spurious helicity dependent mechanism (such as, for example, propagation through a birefringent medium) has affected the relative propagation of the two polarisation states.

So far, the most robust constraints on ξ , derived from time of flight differences, have been obtained from a statistical analysis applied to the arrival times of sharp features in the intensity at different energies from a large sample of GRBs with known redshifts [23], leading to limits $\xi \leq O(10^3)$. Using single objects (generally Blazars or GRBs) it is possible to obtain a stronger, but less robust, constraint of order $|\xi| \leq O(10^2)$ [24].

3.2. Birefringence

According to Eq. (3) LV parameters for left and right circularly polarised photons are of opposite sign. As a consequence, during signal propagation, linear polarisation is

rotated through an energy dependent angle. The difference in rotation angle is

$$\Delta\theta = \xi(k_2^2 - k_1^2)d/2M . \quad (8)$$

The fact that polarised photon beams are indeed observed from distant objects imposes constraints on ξ . A strong constraint, $\xi \lesssim 2 \times 10^{-4}$, has been obtained by looking at UV radiation from distant galaxies [25]. Recently, a claim of $|\xi| \lesssim 2 \times 10^{-7}$ has been made using UV/optical polarisation measures from GRBs [26]. This is currently the strongest constraint on the LV coefficient for photons in the modified QED considered here.

3.3. Photon decay

The decay of a photon into an electron/positron pair is made possible by LV because the photon 4-vector is not null. This process has a threshold which, if $\xi \simeq 0$, is set by the condition

$$k_{th} = (6\sqrt{3}m_e^2M/|\eta_{\pm}|)^{1/3} , \quad (9)$$

where η is the LV parameter for either an electron or a positron. Since, from birefringence $\xi \lesssim 10^{-7}$, the above expression for the photon decay can be used to constrain the electron/positron parameters. In [2] $|\eta_{\pm}| \lesssim 0.2$ was derived using the fact that 50 TeV γ -rays were measured from the CN. This constraint has been tightened to $|\eta_{\pm}| \lesssim 0.05$, thanks to observations of 80 TeV photons by HEGRA [27].

3.4. Vacuum Čerenkov – IC electrons

In the presence of LV the process of Vacuum Čerenkov (VC) radiation $e \rightarrow e\gamma$ can occur. Taking again $\xi \simeq 0$, the threshold energy is given by

$$p_{VC} = (m_e^2M/2\eta)^{1/3} \simeq 11 \text{ TeV } \eta^{-1/3} . \quad (10)$$

Moreover, just above threshold this process is extremely efficient, having a time scale of order $\tau_{VC} \sim 10^{-9}$ s. TeV emission from the CN is usually attributed to the Inverse Compton scattering (IC) of electrons/positrons on background photons (mainly those from synchrotron radiation). These leptons would not be able to produce the observed IC radiation if they were above the VC threshold, because above p_{VC} the VC rate is much higher than the IC scattering rate in the CN.

The observation of 50 TeV photons from the CN implies (by energy conservation) the presence of at least 50 TeV leptons. This leads to the bound $\eta \lesssim 10^{-2}$ for at least one of the four fermion parameters [2]. With the observation of 80 TeV photons by HEGRA [27] the constraint can be strengthened to $\eta \lesssim 3 \times 10^{-3}$ as shown in figure 1 (dashed vertical line in the positive η range).

3.5. Synchrotron radiation

The synchrotron radiation emitted by electrons/positrons spiralling in a magnetic field is strongly affected by LV. In the LI case, as well as in the LV one [2, 28, 29], most of the radiation from an electron of energy E is emitted around a critical frequency

$$\omega_c = \frac{3}{2}eB \frac{\gamma^3(E)}{E} \quad (11)$$

where $\gamma(E) = (1 - v^2(E))^{-1/2}$, and $v(E)$ is the electron group velocity. However, in the LV case, the electron group velocity is given by

$$v(E) = \frac{\partial E}{\partial p} = \frac{p}{E} \left(1 + \frac{3}{2}\eta \frac{p}{M} \right). \quad (12)$$

Therefore, $v(E)$ can exceed 1 if $\eta > 0$ or can be strictly less than the low energy speed of light if $\eta < 0$, resulting in $\gamma(E) \leq E/m_e$ for $\eta \leq 0$. Moreover, if $\eta > 0$, $\gamma(E)$ grows without bound until it diverges at the soft VC threshold (10), which is well below the Planck scale for any $\eta \gg (m_e/M)^2 \approx 10^{-44}$. On the other hand, for any $\eta < 0$, $\gamma(E)$ has a maximum and, hence, the critical frequency has an upper bound, ω_c^{\max} .[§] Then, if synchrotron emission up to some maximal frequency ω_{obs} is observed, one can deduce that the LV coefficient for the corresponding leptons cannot be more negative than the value for which $\omega_c^{\max} = \omega_{\text{obs}}$. This leads to the bound [2, 28]

$$\eta > -\frac{M}{m_e} \left(\frac{0.34 eB}{m_e \omega_{\text{obs}}} \right)^{3/2}, \quad (13)$$

which is strongest when the empirical ratio B/ω_{obs} is minimised. Once again, the CN is the plerion for which the best constraint can be cast.

Making the conservative assumption that the 100 MeV photons detected by γ -ray experiments [33] are produced by synchrotron emission, a lower bound $\eta > -8 \times 10^{-7}$, for at least one η , has been set [2]. For the case of positive η , similar reasoning cannot be applied, because for any positive η a particle can emit all synchrotron frequencies (up to infinity, in principle). Hence, a detailed reconstruction of the emitted spectrum is needed in this case.

3.6. Helicity decay

Although it is not represented in figure 1, this reaction is relevant to our investigation. In the presence of LV, high energy electrons and positrons can flip their helicity with the emission of a suitably polarised photon (Helicity Decay, HD). This reaction does not have a real threshold, but rather an effective one [2]:

$$p_{\text{HD}} = (m_e^2 M / \Delta\eta)^{1/3}, \quad (14)$$

[§] Notice that in our framework the sign of η_{\pm} is undetermined. Conversely in DSR-like scenarios only superluminal parametrisation (i.e. $\eta > 0$) is allowed [30] while in the string-inspired Liouville model of space-time foam [31] such coefficients are exactly zero and only the photon dispersion relation acquires a LV modification. This stresses the importance of a clear choice of framework when discussing this sort of phenomenological constraints (see e.g. [17, 32, 2]).

where $\Delta\eta = |\eta_+ - \eta_-|$, at which the decay lifetime τ_{HD} is minimised. For $\Delta\eta \approx O(1)$ this effective threshold is around 10 TeV. For our purposes it is interesting to note that below threshold

$$\tau_{HD} > \Delta\eta^{-3} (p/10 \text{ TeV})^{-8} 10^{-9} \text{ s}, \quad (15)$$

while above threshold τ_{HD} becomes independent of $\Delta\eta$ [2]. A constraint of $\Delta\eta < 0.4$ has been indirectly inferred in [2] from the photon decay bound $|\eta_{\pm}| < 0.2$.

3.7. An unfinished job

We have seen that while the natural magnitude of the photon and electron coefficients ξ, η_{\pm} would be $O(1)$ if there were one power of suppression by the inverse Planck mass, the coefficients are currently restricted to the region $|\xi| \lesssim 10^{-7}$ by birefringence and $|\eta_{\pm}| \lesssim 10^{-1}$ by photon decay.

Thus, whereas the constraint on the photon coefficient is remarkably strong, the same cannot be said about the LV coefficients of leptons. A constraint on the lepton coefficients of comparable strength is given by the synchrotron limit, but this is not double sided and implies only that the LV coefficient of the population responsible for the CN synchrotron emission cannot be smaller than -8×10^{-7} . Similarly the VC-IC bound $\eta < +3 \times 10^{-3}$ constrains only one lepton population. These statements, although not void of physical significance, cannot be considered constraints on η_{\pm} , since for each of them one of the two parameters $\pm\eta_+$ (and $\pm\eta_-$) will always satisfy the bound.

More can be said by using information obtained from current models of the CN emission, in particular the fact that the CN emission is well fitted by assuming that a single lepton population accounts for both the synchrotron and IC radiation [2]. This implies that at least one of the four pairs $(\pm\eta_{\pm}, \xi)$ must lie in the narrow region bounded horizontally by the dashed lines of the synchrotron and IC bounds and vertically by the birefringence constraint (see figure 1). However, the dashed region limits apply at most to one of the four pairs $(\pm\eta_{\pm}, \xi)$ as we cannot *a priori* exclude that only one out of four populations is responsible for both the synchrotron and IC emission (see again [2] for further details).

It is clear that these simple arguments do not fully exploit the available astrophysical information. A detailed comparison of the observations with the reconstructed spectrum in the LV case, where all reactions and modifications of classical processes are considered, can provide us with constraints on both positive and negative η for the four lepton populations, at levels comparable to those already obtained for the photon LV coefficient. Let us then move to reconsider such information concerning the astrophysical object that so far has proven most effective in casting constraints on the electron/positrons LV coefficients: the CN.

4. The Crab Nebula

The CN is a source of diffuse radio, optical and X-ray radiation associated with a Supernova explosion observed in 1054 A.D., at a distance from Earth of about 1.9 kpc. A pulsar, presumably the neutron star remnant of the explosion, is located at the centre of the Nebula, and is believed to supply both the radiating particles (mostly electrons and positrons) and magnetic fields, as well as the required power, which is somewhat less than the rotational energy loss-rate of the star (the “spin-down luminosity”), of roughly 5×10^{38} erg/s (for a recent review see [34]).

The Nebula emits an extremely broad-band spectrum (covering 21 decades in frequency), produced by relativistic leptons via two major radiation mechanisms: synchrotron radiation from radio to low energy γ -rays ($E < 1$ GeV), and IC scattering for the higher energy γ -rays. The clear synchrotron nature of the radiation below ~ 1 GeV, combined with a magnetic field strength of the order of $B \approx 100 \mu\text{G}$ implies, when exact LI is assumed, the presence of relativistic leptons with energies up to 10^{16} eV. Their gyro period is comparable to the synchrotron cooling timescale, implying an acceleration rate close to the maximum estimated for shock-based mechanisms (e.g. [35]).

The appearance of the CN depends on the observational wavelength: in X-rays it is ellipsoidal, with angular dimensions $2' \times 3'$ (corresponding to $\sim 1.2 \times 1.8$ pc at the Crab distance). In the centre it displays a jet-torus structure in the X-ray and optical bands. In the radio, this feature is less apparent, and the Nebula is more extended, with a dimension of about $6'$ [36]. Low frequency (radio) observations allowed also the discovery of a number of structures on subarcsecond scale, such as wisps, ripples, jets and arcs. Interestingly, most of these substructures are seen also in the optical [37] and X-rays [38].

In the frequency band ranging from radio to optical, the overall emission spectrum of the CN has an extremely regular power-law shape, with spectral index $\alpha_s = -0.27 \pm 0.04$ ($F \propto E^{\alpha_s}$). The X-ray spectrum integrated over the whole Nebula is also well represented by a power-law with spectral index $\alpha_s \approx -1.1$ in the energy range 1-20 keV [39]. In the 0.5-8 keV band, the spectrum softens as the distance from the shock position in the Nebula increases [39], with the spectral index passing from -0.9 in the inner region to about -2.0 in the outer one. This result is confirmed by observations with the XMM-Newton satellite [40], and is consistent with the overall expectations from the spherically symmetric magneto-hydro-dynamic model by [41] (although a detailed analysis reveals effects that may be due to non-radial components of the flow velocity [42]).

The γ -ray flux measured by EGRET [33] between 50 MeV and 10 GeV matches well the extrapolation from the 50–500 MeV range [43], which has been interpreted [44] as an extension of the synchrotron spectrum from lower energies. The observed hardening of the spectrum above 500 MeV was indeed predicted by [44], as due to the increased contribution of IC emission.

Very high energy γ -rays from the CN were detected in the pioneering observations

by Whipple [45], and, since then, by several Imaging Atmospheric Čerenkov Telescopes (IACT) (see, for example, [27, 46, 47, 48]) and Extensive Air Shower (EAS) detectors. The HEGRA stereoscopic IACTs observed the CN between 500 GeV and 80 TeV [27]. The energy spectrum (with an overall uncertainty of $\sim 15\%$) is well approximated by a pure power-law with $\alpha_s \sim -1.62$. Remarkably, the data show a 2.7σ excess even at 86 TeV. Its position was determined to be shifted by about $12''$ (though with a systematic uncertainty of $25''$) to the west of the nominal position of the pulsar and consistent with the centroid position of the X-ray emitting nebula. The extension of the TeV excess (less than $3'$ at 10 TeV) excludes a strong contribution from the still undetected outer shock of the expanding supernova remnant and is compatible with leptons being accelerated in the proximity of the termination shock and then cooled by the synchrotron/IC processes. The data by HEGRA are also compatible with the expected softening of the spectrum at high energies ($E \geq 70$ TeV). This behaviour is confirmed by more recent HESS observations [48]: the combined data sets for the differential spectrum are best fitted by a power-law (with slope $\alpha_s \sim -1.39$) with an exponential cut-off at $14.3 \pm 2.1 \pm 2.8$ TeV, rather than a pure power-law. Though the maximum lepton energy is model dependent, the fact that photons with $E \gtrsim 10$ TeV have been detected from the CN is unambiguous evidence of the acceleration of particles beyond 100 TeV. Let us stress that this statement has to be considered robust also in our test theory, in which energy-momentum conservation still holds.

4.1. Theoretical model

From the theoretical point of view, the CN is one of the most studied objects in astrophysics. However, in spite of more than 30 years of theoretical efforts, important details of the interactions between the pulsar wind and the synchrotron nebula are still missing. The current understanding is based on a spherically symmetric magneto-hydrodynamic (MHD) model presented in two seminal papers by Kennel & Coroniti [41, 49], that accounts for the general features seen in the spectrum. In their model, the synchrotron nebula is powered by the relativistic wind of cold electrons generated by the pulsar and terminated by a standing reverse shock wave at $r_S \simeq 0.1$ pc [50], due to the balance of the ram pressure of the flow with the pressure of the outer nebula. Kennel & Coroniti found a stationary solution in which the particle flow evolves adiabatically in the magnetised nebula. The magnetisation of the flow is parametrised by $\sigma = B^2/4\pi\gamma\rho$, which is the ratio between the magnetic and the kinetic energy density in the flow (ρ being the density). The value of σ is determined by the conditions at the outer boundary of the Nebula. In fact, since the postshock flow has to match the velocity of the material at the interface between the Nebula and the remnant, which is non-relativistic, and a lower bound to the flow speed is given by $v \gtrsim \sigma/(1+\sigma)$ [41], it turns out that σ has to be small, of order 10^{-3} [51]. However, the magnetic field is clearly dynamically important in the Nebula, because it is responsible for its ellipsoidal shape [52, 53]. Therefore, the value of σ cannot be substantially less than 10^{-3} .

Observations of the radio and optical brightness distributions confirm that the magnetic field, which is to a good approximation toroidal, is not constant in the CN, but increases in the central region ($r \leq 0.5$ pc) with distance from the pulsar. Its behaviour as a function of radius downstream of the shock front (shown in figure 2) is determined initially by the gas pressure, which remains almost constant. Because the

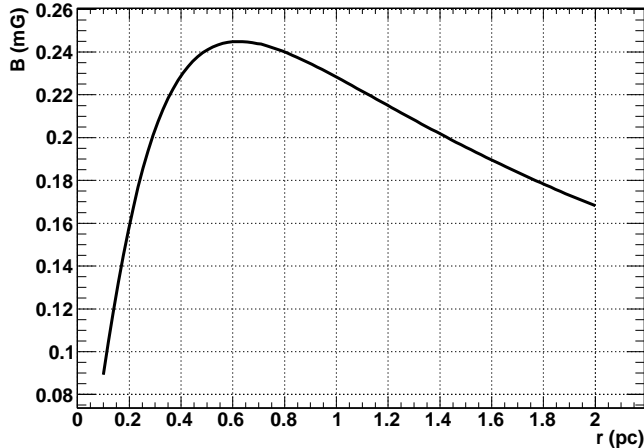


Figure 2. Magnetic field profile following Kennel & Coroniti, assuming the best fit value $\sigma = 0.003$ and the reverse shock wave position $r_S \approx 0.1$ pc.

gas behaves almost adiabatically, the density is also initially constant, and the radial velocity decreases as $1/r^2$, leading to an increase in the frozen in toroidal magnetic field $B(r)$. When $B(r)$ approaches the equipartition value of 0.3 mG [54] and starts to play a role in the dynamics of the flow, it ceases to grow and then falls off with increasing distance.

5. The Crab model revisited

Because we consider a LV version of electrodynamics, we must check whether this introduces modifications into the model of the CN and, if so, what effects it produces.

The observed spectrum of the CN is the composite result of several processes, as sketched in sec. 4. The way LV affects the physics of the CN is basically twofold. On the one hand, classical processes, such as acceleration, synchrotron emission and IC scattering, can be modified. On the other hand, new processes (such as VC or HD) come into play. On general grounds, we expect both the modifications and the new processes to be important at energies above $(m_e^2 M / \eta)^{1/3} \approx 10 \text{ TeV} \eta^{-1/3}$, which is the typical scale of threshold for almost all LV features. We now investigate how the processes at work in the CN would appear in a LV framework.

5.1. Acceleration

Several mechanisms have been suggested for the formation of the spectrum of energetic leptons in the CN. The spectrum is unusual in the sense that most of the leptons are concentrated at low energy, $E \sim 100$ MeV, whereas the energy density contained in each decade of particle energy peaks at about 1 TeV. Above this energy, the spectrum appears to fall off roughly as $E^{-2.2}$. Most of the uncertainty concerning the acceleration mechanism refers to the low energy part of this distribution, $E \leq 1$ TeV. The power-law spectrum of high energy particles is usually interpreted in terms of the first order Fermi mechanism operating at the ultra-relativistic termination shock front of the pulsar wind, since, in the simplest kinematic picture, this mechanism predicts a power law index of just the right value [34].

In this picture, electrons and positrons acquire energy by crossing and recrossing a shock front that propagates in a magnetised medium. In between crossings, they are continually deflected by the random magnetic field present in the medium, and may, therefore, reverse their direction of travel. The magnetic deflections do not change the particle energy as seen from a reference frame travelling with the plasma. However, when a particle crosses a shock, it is exposed to magnetic fluctuations embedded in an approaching plasma flow. These increase the particle energy whenever it is deflected back to the shock front.

The cycle of shock crossing and recrossing can be accomplished many times, and each time the particle has a finite probability of escaping from the vicinity of the shock front into the downstream medium, never to return. The competition between energy gain and escape leads to a scale-free power-law spectrum of accelerated particles. The power-law index depends on the shock compression ratio, and, in the relativistic case, on the angular dependence of the deflection process. In the ultra-relativistic case, a variety of scattering laws have been tested by different methods [55, 56], all of which appear to give an index in the range -2 to -2.3 , close to the asymptotic value of -2.23 , which can be derived semi-analytically for isotropic diffusion in angle [57].

5.1.1. The Fermi mechanism in the LV scenario. From the LV point of view, the important issue about the Fermi mechanism is that its scale-free nature rests purely on the angular distribution of the particles at the shock front. This determines both the escape probability P_{esc} of a particle that crosses from upstream to downstream, as well as the average change in particle Lorentz factor $\langle \Delta\gamma \rangle$. The latter is found by convolving the Lorentz boost into the upstream plasma frame with the return boost, averaged in each case over the angular distribution function. Both P_{esc} and $\langle \Delta\gamma \rangle$ are independent of the length scale associated with the scattering process – an increase in the scattering mean free path simply produces a longer time interval between crossings, and a slower fall-off of the particle distribution with distance from the shock, but changes neither the angular distribution at the shock front, nor the escape probability.

In the LV picture, both the particle energy and Lorentz factor enter into the

computation of the trajectory. But, given that the angular distribution is not a function of either of these, the spectrum produced by the first order Fermi mechanism depends on the Lorentz factor alone, through the quantity $\langle \Delta\gamma \rangle$. On the other hand, the maximum energy E_c to which the process can accelerate particles may depend on loss processes as well as on the time interval between shock crossings, which controls the acceleration rate. In the standard LI case, E_c is essentially determined either by setting the particle gyro radius to equal the size of the system, or the acceleration rate (which scales with the gyro frequency) to equal the loss rate. In each case, a condition on the particle energy rather than the particle Lorentz factor results. In the CN, if we phenomenologically model the cut-off at E_c as an exponential, we expect a particle spectrum in the high energy region, $E > 1$ TeV, of the form

$$n(E) \propto \gamma(E)^{-p} e^{-E/E_c} \quad (16)$$

with $p \approx 2.4$ and $E_c \approx 2.5 \times 10^{15}$ eV.||

Then, we can safely deal with the electron/positron distributions inferred by [49, 58], paying attention to replace the energy with the Lorentz boost factor in the expressions given by [58]. Of course, as we mentioned, the cut-off of the spectrum results in a condition on the particle energy rather than its boost.

5.1.2. The role of Vacuum Čerenkov emission. However, in the LV theory there are additional mechanisms that can influence E_c because the modified dispersion relations that we consider allow processes that are otherwise forbidden. In particular, the VC emission, due to its extreme rate above threshold, can produce a sharp cut-off in the acceleration spectrum (let us remind that above threshold $\tau_{VC} \sim 10^{-9}$ s, to be compared with the acceleration time scale $\tau_{acc} > 10^3$ s).¶

One might expect that the VC radiation emitted by particles above threshold should produce some modification in the spectrum. However, since the photon LV parameter ξ has been independently constrained to be very small, the VC process occurs in the soft regime [2]. In this regime the emitted photon carries away a small fraction of the electron energy, being at most in the optical/UV range. Moreover, the emitting leptons are just in the high energy tail of the spectrum, so that they are few in number, compared to the optical/UV emitting ones. Therefore, the contribution of VC to the CN spectrum in the optical/UV range should be negligible.

|| Super-exponential cut-off spectral shapes do not lead to significant differences in the output spectrum. For this reason we considered a simple exponential cut-off, which also gives the best fit to the data.

¶ An order of magnitude estimate of a lower limit to the acceleration timescale can be obtained by assuming the particle doubles its energy whenever it completes a cycle of crossing and recrossing the shock front. Since magnetic fields bend the particle trajectory to make it do this, a lower limit to the cycle time is given by the gyro period (magnetic turbulence may make the particle diffuse, enhancing the time needed to complete a cycle). The acceleration timescale is, therefore, $\tau_a > \gamma m_e / eB \approx 1.1 \times 10^3$ s $(E/1 \text{ TeV}) (B/100 \text{ } \mu\text{G})^{-1}$.

5.1.3. The role of Helicity Decay and spin precession. A more subtle effect in the determination of the emitting particle spectrum is given by the HD process. At high energies, the electron and positron states have well-defined helicity and the LV coefficients η_{\pm} are different depending on the particle helicity.

As discussed, the HD rate peaks at energies around p_{HD} (see (14)). Below p_{HD} the rate increases with energy and depends on $\Delta\eta$, while above p_{HD} it decreases independently of η [2]. The expressions (10) and (14) for p_{VC} and p_{HD} , respectively, show that at most $p_{\text{HD}} \gtrsim p_{\text{VC}}$ for $\Delta\eta \lesssim \eta$ (otherwise $\Delta\eta \ll \eta$ and $p_{\text{HD}} \gg p_{\text{VC}}$). Since the VC emission acts as a hard cut-off on the accelerated particles, in our scheme the HD process will occur only in the regime $p \lesssim p_{\text{HD}}$, where the (not yet maximised) rate grows with energy.

However, in order to understand whether the HD is effective, one has to compare its typical time scale τ_{HD} , as given in eq. (15), with the other relevant ones. In particular, a competitive process is the precession of the spin of a particle moving in a magnetic field. According to [59] in the LI case (it can be checked that this is still valid in the LV case, without any modification, to within 10^{-14}) the rate of change of the spin orientation with respect to the instantaneous direction of motion of the lepton in the laboratory frame is ⁺

$$\frac{d\theta}{dt} \equiv \omega_{\text{SR}} = \frac{e}{m_e} \frac{g-2}{2} B, \quad (17)$$

where $(g-2) = \alpha/\pi$ represents the anomalous magnetic moment of the lepton and a constant magnetic field B is assumed. (Indeed it is expected that the magnetic field in the CN is constant only over some typical correlation length after which it reverses sign. For our purposes, however, it is the rate of spin-rotation that is relevant, rather than its direction.)

The spin rotation will effectively prevent helicity decay if the spin precession rate is faster than the time needed for LV induced effect. Therefore, the HD will play a role in spite of the spin precession whenever the condition $\omega_{\text{SR}}\tau_{\text{HD}} \ll 1$ is met.

According to (15) and (17) this condition translates into

$$p_{\text{HD}}^{(\text{eff})} \gtrsim 930 \text{ GeV} \left(\frac{B}{0.3 \text{ mG}} \right)^{1/8} |\Delta\eta|^{-3/8}. \quad (18)$$

Electrons and positrons with $E > p_{\text{HD}}^{(\text{eff})}$, can therefore be found only in the helicity state that corresponds to the lowest value of η_{\pm} . Correspondingly, the population of greater η will be sharply cut off above $p_{\text{HD}}^{(\text{eff})}$ while the other will increase.

⁺ A comment is in order here as, in principle, there could be interference between spin precession and HD. However, assuming a static magnetic field, during spin precession the electron energy is constant while HD implies the emission of a photon, leading to non conservation of the electron energy. Therefore they cannot interfere. Moreover, if a constant timelike vector u^{μ} is used to “parametrise” Lorentz symmetry violation, a term like $\bar{\psi}\gamma_{\mu}u^{\mu}\psi$ can appear in the Lagrangian, which mimics the usual electro-magnetic interaction term. However, as long as u^{μ} is constant, it cannot give rise to magnetic-like interactions.

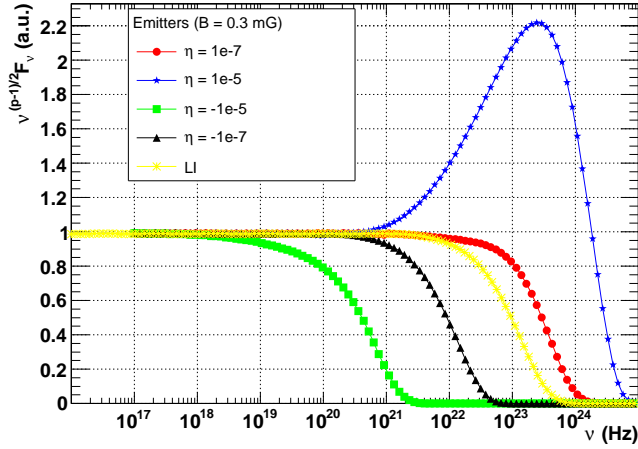


Figure 3. Modifications occurring due to LV in the synchrotron spectrum produced by a power-law distribution of leptons. The spectrum is normalised to a LI one without cut-off.

Finally, the HD process implies the emission of a suitably polarised photon. However, this has no consequences for the observed spectrum, since the mean photon energy (for $\Delta\eta \sim 10^{-6}$) is well within the radio band, where the synchrotron spectrum, emitted by an overwhelmingly large number of low energy electrons, is dominant. We refer the reader to Appendix A for a detailed discussion.

5.2. More on synchrotron radiation

The main modifications of the synchrotron emission process in presence of LV have already been presented in Section 2. Let us however consider them in more detail.

There is a fundamental difference between particles with positive or negative LV coefficient η . If η is negative the group velocity of the electrons is strictly lower than the (low energy) speed of light. This implies that, at sufficiently high energy, $\gamma(E)_- < E/m_e$ for all E . As a consequence, the critical frequency $\omega_c^-(\gamma, E)$ is always lower than the LI one, and so the exponential cut-off of the LV synchrotron spectrum will be at lower frequencies than in the LI case, as illustrated in figure 3.

On the other hand, particles with a positive LV coefficient can be superluminal and, therefore, $\gamma(E)$ increases more rapidly than E/m_e , reaching infinity at a finite energy, which corresponds to the threshold for soft VC emission.* Therefore, the critical frequency is also larger than that found in the LI case, and the spectrum will show a characteristic hump due to the enhanced ω_c (see figure 3).

The final remark concerns the characteristic synchrotron loss timescale, defined as $\tau_{cool} = E/(dE/dt)$. The classical result for an electron spiralling in a given magnetic

* Of course such an infinity will be automatically “regulated” by the fact that, as the electron approaches the threshold, its energy loss rate will at some point exceed its rate of energy gain, thus preventing further acceleration.

field is

$$\frac{dE}{dt} = -\frac{2e^4}{3m_e^2}\gamma^2 B^2 v^2 \sin^2 \phi, \quad (19)$$

where ϕ is the pitch angle and $\gamma = E/m_e$. As the electron loses most of its energy at frequencies around the critical one, a comparable expression for the LV case can be written as

$$\frac{dE}{dt} \sim \frac{\omega_c}{\Delta t} \sim \frac{\gamma^4}{E^2}, \quad (20)$$

where we have used eq. (11) and the fact that the typical emission time at ultra-relativistic energy is $\Delta t = 2\pi R(E)/\gamma$, with $R(E) = E/eB$. The numerical factor in front of expression (21) can be fixed by fitting the energy loss rate at low energies, where $\gamma = E/m_e$.

One might wonder if this modified rate could alter the effectiveness of the acceleration mechanism in producing the highest energy leptons. In fact, while for $\eta < 0$ this is not an issue, for $\eta > 0$ one expects the rate to grow much faster than the LI one for sufficiently high energies. Nonetheless it is easy to see that appreciable deviations from the LI rate (19) occur at energies $E \gtrsim 8 \text{ TeV}/\eta^{1/3}$, i.e. in the proximity of the VC threshold. Therefore the effective cut-off on the spectrum of the injected particles is not significantly lowered by the synchrotron cooling in the LV case.

5.3. IC radiation

The IC process is not strongly affected by LV. At the kinematic level all LV terms intervene at a level of $< 10^{-11}$ at $E \lesssim 1 \text{ PeV}$, whereas the cross section should be corrected by adding factors proportional to p^3/M_{Pl} and, therefore, the LV contribution is again suppressed at the same level. Since the IC and synchrotron emission mechanisms can be thought as being due to the scattering of a lepton off a real or a virtual photon respectively [60], one may wonder why the synchrotron is much affected by LV while the IC is not.

The main difference between the two processes is that IC scattering involves the interaction between a real lepton and a real photon, whereas the synchrotron process involves a virtual photon of the magnetic field in which the lepton is spiralling. In the former case, the interaction is effective no matter what the photon energy is. In the latter case, however, the reaction is more subtle. An electron spiralling in a static magnetic field can exchange momentum but not energy with the field, since it is static. Moreover, the exchanged momentum is such that the electron accelerates and describes a spiral trajectory. Therefore, a synchrotron emitting electron does not interact with all possible virtual photons, but only with those that provide it with the required momentum transfer. In a sense, this is a sort of a resonant process, where the resonance is dependent not only on the electron energy, but also on its velocity.

Therefore, the admixture of dynamical and kinematic variables in the synchrotron emission process makes it much more sensitive to LV compared IC scattering, where

only energetic considerations matter: this is another example of the fact that, in LV reasoning, velocity (or boost in γ) and energy are not quite the same concept.

6. Results

In order to constrain our test theory by exploiting the information contained in broad band observations of the CN, we adopt the following strategy.

First of all we construct a numerical algorithm[‡] that calculates in full generality, for any set of LV parameters, the synchrotron emission from a distribution of leptons, according to the model of the CN presented in section 4 and taking into account all the processes discussed in section 5. Of course, the LI model is recovered by simply setting $(\eta_+, \eta_-) = (0, 0)$. Then, we fix most of the model parameters (magnetic field strength and particle energy density) so as to match observations from radio to soft X-rays, i.e. in a regime where the LV terms here considered are not expected to produce significant effects.

This procedure leads to model parameters (and a LI spectrum) which are in agreement with those providing the best fit to the data in [58]. We report here the most relevant parameters, namely $p = 2.4$ as the spectral index and $E_c = 2.5$ PeV as the high energy cut-off of the freshly accelerated wind leptons.^{††} The same parameters are known to be able to reproduce the IC part of the CN spectrum in the LI case [58]. Given that the IC reaction is basically unaffected by LV, agreement with the high energy data will hold also for non zero LV coefficients. Of course this also implies that, at least with current data accuracy, the IC cannot be used to improve on the constraints obtainable from the synchrotron part of the spectrum.

6.1. Spectra

The general features of the spectra produced by our numerical computation are illustrated in figure 4 for $\eta_+ \cdot \eta_- > 0$ (left panel) and $\eta_+ \cdot \eta_- < 0$ (right panel) with η_+ assumed to be positive for definiteness. It is clear that only these two cases are really different: in fact, the one with both η_{\pm} negative is the same as the $(\eta_+ \cdot \eta_- > 0, \eta_+ > 0)$ case, while that with the signs scrambled is equivalent to the case $(\eta_+ \cdot \eta_- < 0, \eta_+ > 0)$. This is simply due to the fact that positron coefficients are related to electron coefficients through $\eta_{\pm}^{af} = -\eta_{\mp}^f$ (see section 2).

One can easily see that in the LI case the data are reasonably fitted (as in [58]) and that the LV effects indeed appear at the expected energy scales. Hence the procedure of fixing the free (LI) parameters from the low energy observations is well defined.

The main difference between the left and right panels of figure 4 consists in the fact that in the first case ($\eta_+ \cdot \eta_- > 0$) only a population with positive η survives to the HD,

[‡] The code is written in C++ and takes great advantage of many tools provided by the ROOT package, see <http://root.cern.ch>

^{††} Note however, that in the LV case the cut-off energy of the injected particles can be lowered by the VC process.

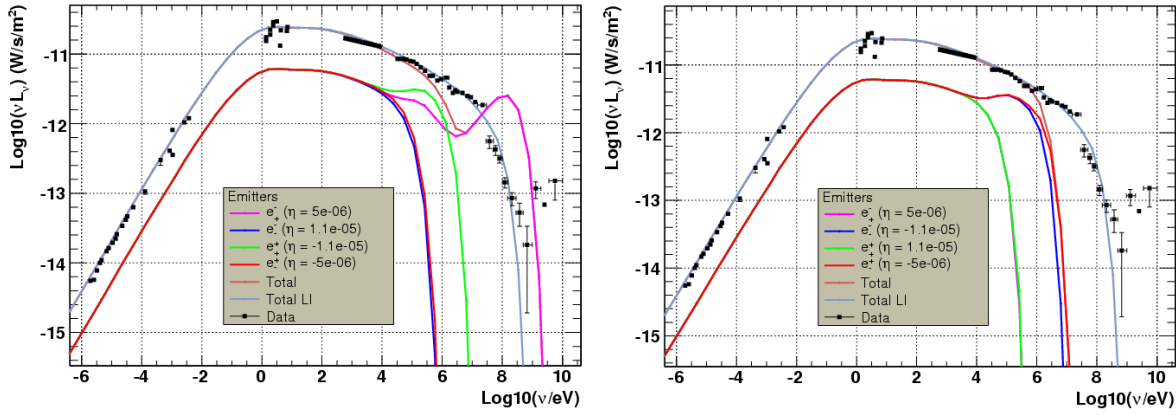


Figure 4. Comparison between observational data, the LI model and a LV one with $\eta_+ \cdot \eta_- > 0$ (left) and $\eta_+ \cdot \eta_- < 0$ (right). The values of the LV coefficients are reported in the inserted panels and are chosen in order to show the salient features of the LV modified spectra. The leptons are injected according to the best fit values $p = 2.4$, $E_c = 2.5$ PeV. The individual contribution of each lepton population is shown.

while in the opposite case ($\eta_+ \cdot \eta_- < 0$) only a population with negative η does. This has consequences for the total synchrotron spectrum. In particular, the right panel of figure 4 shows a sharp cut-off since the high energy emission in this case is produced by a population with negative η which, as discussed, has an upper bounded ω_c . On the other hand, for $\eta_+ \cdot \eta_- > 0$ (left panel of figure 4) a pronounced feature appears with a dip followed by a hump. The dip is due to the combination of two effects: the population is decaying with increasing energy, while the critical frequency ω_c is growing faster than “usual” with energy. Hence, at some point the spectrum has a minimum and then starts growing. Since, however, the population of the highest energy leptons (responsible for the γ -ray part of the synchrotron spectrum) is decaying very rapidly, the flux does, in the end, also decay. This effect is responsible for the hump.

Finally, one might wonder if in this last case it is possible to reproduce the high energy synchrotron emission even with $E_c \lesssim 1$ PeV. However, this would require so high values of the LV parameters (of order $10^{-4} \div 10^{-3}$) that the resulting spectrum would show a feature in hard-X/soft γ -rays incompatible with the observations.

6.2. Constraints

In order to evaluate the constraints in an objective and quantitative manner, we present a χ^2 analysis of the agreement between models and data. Figure 5 and figure 6 show the contour levels of the reduced χ^2 for the two cases $\eta_+ \cdot \eta_- > 0$ and $\eta_+ \cdot \eta_- < 0$, respectively. Constraints at 90%, 95% and 99% Confidence Level (CL) correspond, respectively, to $\chi^2 > 8$, $\chi^2 > 10$, $\chi^2 > 13.5$. The minimum value of χ^2 we obtain is ~ 3.6 (see [61] for more complete information). From figure 5 and figure 6 we conclude that the LV parameters for the leptons are both constrained, at 95% CL, to be $|\eta_{\pm}| < 10^{-5}$.

Our statistical analysis shows that there are values of the pair (η_+, η_-) that

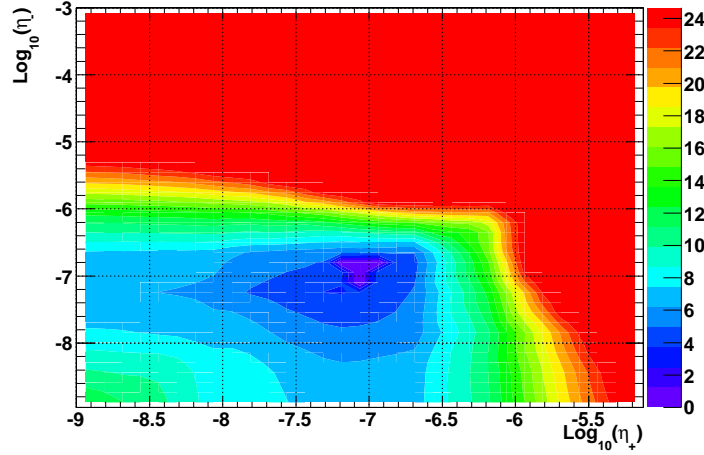


Figure 5. Contour plot of the reduced χ^2 versus η_+ and η_- , in the case $\eta_+ \cdot \eta_- > 0$.

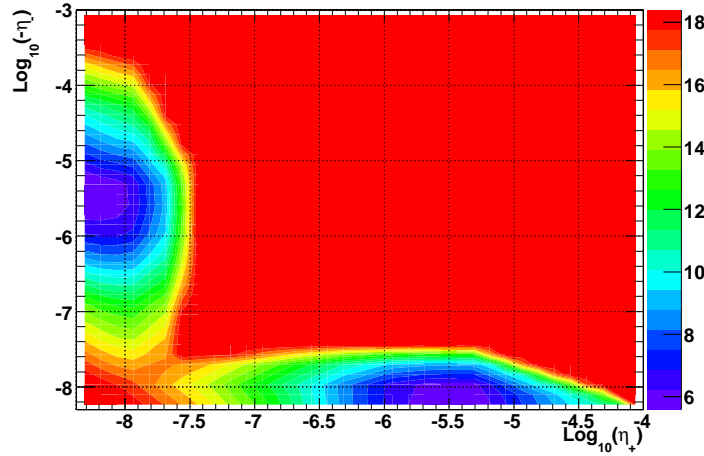


Figure 6. Contour plot of the reduced χ^2 versus η_+ and η_- , in the case $\eta_+ \cdot \eta_- < 0$.

provide a better fit of the CN data than the LI model. In particular, for $(\eta_+, \eta_-) \sim (5.2 \times 10^{-8}, 5.7 \times 10^{-8})$ it is possible to reproduce (see figure 7) some features in the MeV range that are not found in the standard model. Of course, while it is possible to explain these features by introducing new components into the LI model, at the moment it seems that such alternatives would imply some sort of departure from the standard model of the CN emission (for example, [58] postulate the existence of an additional population of emitting particles, with a Maxwellian distribution).

Putting aside for the moment alternative (Lorentz invariant) models, something more can be said about the above result by further investigating its statistical significance. This can be accomplished by assessing the significance of the difference between the χ^2 values of the best fit (LV) model and the standard LI one given that the extra two degrees of freedom characterising the LV case obviously allow for better

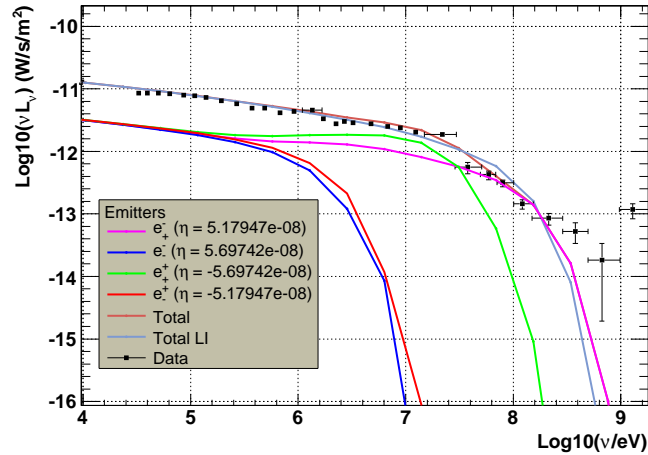


Figure 7. Best fit LV spectrum compared to the LI one.

fits. (Unfortunately, it is not possible to assess the probability to find the best fit value of the LV parameter η given our ignorance of its theoretical expected magnitude or prior distribution.) This can be accomplished using the so called F-test [62]. We find a value of 1.11 for the F-variable, from which we conclude that the LI model and the best fit LV model are statistically indistinguishable at 95% CL. The critical value of the F-variable, for which the models would indeed be distinguishable, is 1.67, and the significant improvements in the 40 – 250 MeV data expected from the up-coming GLAST experiment may enable this value to be reached.

7. Conclusions

We have studied how relaxing the assumption of exact Lorentz invariance (within the framework set up in [18]) influences the electromagnetic output of astrophysical source models. In general, the most important effects are those related to modifications of the particle dispersion relations, which affect their propagation and their interactions.

Starting from the most accurate theoretical model of the CN [49, 58], and taking into account the LV contributions of *all* the electron/positron populations, we reproduce the observed synchrotron spectrum. To do this, one must reconsider LI “biases”. Concerning the acceleration process, we give arguments according to which the particle Lorentz boost, rather than energy, enters in the acceleration spectrum. Moreover, we study the effect of VC emission and HD on the emitting particle distribution.

The synchrotron, as well as the IC, processes are discussed and the spectrum emitted by an arbitrary distribution of leptons, taking into account all the subtleties occurring in LV reasoning, is calculated numerically. In this way *both* η_{\pm} can be constrained by comparing the simulated spectra to the observational data. The χ^2 statistics sets 90% and 95% CL exclusion limits at $|\eta_{\pm}| < 10^{-6}$ and $|\eta_{\pm}| < 10^{-5}$, respectively. The resulting state-of-the-art constraints are shown in figure 8.

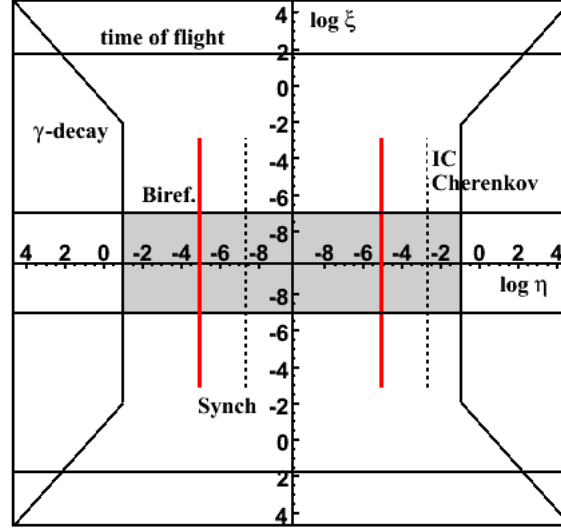


Figure 8. Updated overview of the constraints. The new allowed region of the parameter space is now the grey region bounded vertically by the birefringence constraint $\xi < O(10^{-7})$ and horizontally by the red lines representing the synchrotron constraint, $|\eta_{\pm}| < O(10^{-5})$, discussed here.

The GLAST observatory is likely to achieve a significant step forward. An order of magnitude estimate of the improvement can be obtained by considering its sensitivity, which is ~ 30 times better than that of EGRET in the relevant energy range. Assuming that GLAST will observe the CN at least as long as EGRET did (a very conservative assumption), measurement errors in the 10 MeV-500 MeV band will be statistically reduced by roughly a factor of ~ 5 . A constraint of order 10^{-6} at 99% CL (10^{-7} at 95% CL) would thus be within reach.

As a final remark, we would like to stress that the very tight constraints achieved here on our test theory [18, 22] show the remarkable potential of this approach and suggest that similar studies should be undertaken for other plausible theoretical frameworks. For example, if one is not willing to accept CPT violation in quantum gravity, then the QED dimension 5 LV operators considered here would be forbidden and dimension 6 operators (corresponding to $O(p^2/M^2)$ suppressed terms in the dispersion relations) should be considered. In this direction, on the one hand a theoretical development of the theory is much needed as we still lack a formalisation of the QED extension in this case (including the consideration of possible effects on lower dimensional operators which could play a crucial role in casting constraints). On the other hand, more accurate, higher energy and possible new observations will be needed in order to overcome the larger suppression of such higher order LV terms.

Acknowledgments

We are grateful to Ted Jacobson and David Mattingly for many fruitful discussions and the hints they gave us. We also wish to thank F. Aharonian and P. Blasi for some useful questions and remarks which helped improving the clarity of the paper. The Italian MIUR is acknowledged for financial support.

Appendix A. Comments on Helicity Decay

In order to understand what is the typical energy of the photon emitted during the HD, we sketch here an estimate. An incoming electron with 4-momentum p^μ and LV parameter η_1 decays into another electron with 4-momentum q^μ and LV coefficient η_2 plus a photon of 4-momentum k^μ , whose angle with respect to the direction of motion of the primary electron is θ . Since $\xi < 10^{-7}$ we set $\xi = 0$.

Therefore, the dispersion relations for the particles involved are

$$E_p^2 = m^2 + p^2 + \eta_1 \frac{p^3}{M}, \quad E_q^2 = m^2 + q^2 + \eta_2 \frac{q^3}{M}, \quad \omega^2 = k^2. \quad (\text{A.1})$$

The conservation of energy-momentum $p^\mu = q^\mu + k^\mu$ implies, when the ultra relativistic approximation is made for $E_q/q \approx 1 + m^2/(2q^2) + \eta_2 q/(2M)$, that

$$\eta_1 \frac{p}{M} = \eta_2 \frac{p}{M} \alpha(z, \theta)^3 + 2z \left(\alpha(z, \theta) + \frac{m^2}{2p^2 \alpha(z, \theta)} + \eta_2 \frac{p}{2M} \alpha(z, \theta)^2 - \cos \theta + z \right) \quad (\text{A.2})$$

where $z = \omega/p$ and $\alpha(z, \theta) = \sqrt{1 - 2z \cos \theta + z^2}$. If $z \ll 1$ (we will see that this assumption is justified *a posteriori*),

$$\Delta \eta \frac{p}{M} \approx z \left(\frac{m^2}{p^2} + 2(1 - \cos \theta) - 3\eta_2 \frac{p}{M} \cos \theta \right), \quad (\text{A.3})$$

where $\Delta \eta \equiv \eta_1 - \eta_2$ and whose solution is

$$z(\theta, p) = \frac{\Delta \eta p^3 / M}{m^2 + 2p^2(1 - \cos \theta) - 3\eta_2 p^3 / M \cos \theta}. \quad (\text{A.4})$$

If far from the VC threshold (10) (as in the cases considered in this paper) one can safely neglect the last term in the denominator of (A.4), finding

$$z(\theta, p) = \frac{\Delta \eta p^3 / M}{m^2 + 2p^2(1 - \cos \theta)}. \quad (\text{A.5})$$

From an experimental point of view, the angle θ is unobservable. Hence, (A.5) has to be averaged over the angular distribution of the emitted photons. According to [2], we assume that, at lowest order, the matrix element governing this process is angle independent. Therefore, the mean photon energy is ($x \equiv \cos \theta$ and redefine $z(\theta, p) \rightarrow z(\cos \theta, p)$)

$$\bar{z}(p) = \frac{\int_{-1}^1 dx z(x, p)}{\int_{-1}^1 dx} = \Delta \eta \frac{p}{2M} \ln \left(2 \frac{p}{m} \right). \quad (\text{A.6})$$

Assuming a typical value $\Delta\eta = 10^{-6}$, from (18) $p_{\text{HD}}^{(\text{eff})} = 160$ TeV. Equation (A.6) then implies that $\bar{z}(p_{\text{HD}}^{(\text{eff})}) = 1.7 \times 10^{-19}$, *i.e.* $\bar{\omega} \simeq 2.8 \times 10^{-5}$ eV, well within the radio band.

References

- [1] D. Mattingly, Living Rev. Rel. **8**, 5 (2005)
- [2] T. Jacobson, S. Liberati and D. Mattingly, Annals Phys. **321** (2006) 150 [arXiv:astro-ph/0505267].
- [3] G. Amelino-Camelia, arXiv:gr-qc/0309054.
- [4] L. Smolin, arXiv:hep-th/0605052.
- [5] V. A. Kostelecky and S. Samuel, Phys. Rev. D **39**, 683 (1989).
- [6] G. Amelino-Camelia, J. R. Ellis, N. E. Mavromatos, D. V. Nanopoulos and S. Sarkar, Nature **393**, 763 (1998).
- [7] R. Gambini and J. Pullin, Phys. Rev. D **59**, 124021 (1999).
- [8] S. M. Carroll, J. A. Harvey, V. A. Kostelecky, C. D. Lane and T. Okamoto, Phys. Rev. Lett. **87**, 141601 (2001).
- [9] J. Lukierski, H. Ruegg and W. J. Zakrzewski, Annals Phys. **243** (1995) 90 [arXiv:hep-th/9312153].
- [10] G. Amelino-Camelia and S. Majid, Int. J. Mod. Phys. A **15** (2000) 4301 [arXiv:hep-th/9907110].
- [11] C. P. Burgess, J. Cline, E. Filotas, J. Matias and G. D. Moore, JHEP **0203**, 043 (2002).
- [12] C. Barcelo, S. Liberati and M. Visser, “*Analogue gravity*,” Living Rev. Rel. **8**, 12 (2005). [arXiv:gr-qc/0505065].
- [13] M. Roth and f. t. A. Collaboration, arXiv:0706.2096 [astro-ph].
- [14] R. Abbasi *et al.* [HiRes Collaboration], arXiv:astro-ph/0703099.
- [15] G. Amelino-Camelia, Int. J. Mod. Phys. D **11** (2002) 35 [arXiv:gr-qc/0012051].
- [16] G. Amelino-Camelia, Phys. Lett. B **510**, 255 (2001) [arXiv:hep-th/0012238].
- [17] G. Amelino-Camelia, New J. Phys. **6**, 188 (2004) [arXiv:gr-qc/0212002].
- [18] R. C. Myers and M. Pospelov, Phys. Rev. Lett. **90** (2003) 211601 [arXiv:hep-ph/0301124].
- [19] <http://glast.gsfc.nasa.gov/>
- [20] P. A. Bolokhov and M. Pospelov, arXiv:hep-ph/0703291.
- [21] O. W. Greenberg, Phys. Rev. Lett. **89** (2002) 231602 [arXiv:hep-ph/0201258].
- [22] T. A. Jacobson, S. Liberati, D. Mattingly and F. W. Stecker, Phys. Rev. Lett. **93**, 021101 (2004) [arXiv:astro-ph/0309681].
- [23] J. R. Ellis, N. E. Mavromatos, D. V. Nanopoulos, A. S. Sakharov and E. K. G. Sarkisyan, Astropart. Phys. **25**, 402 (2006).
- [24] S. D. Biller *et al.*, “Limits to quantum gravity effects from observations of TeV flares in active galaxies,” Phys. Rev. Lett. **83**, 2108 (1999) [arXiv:gr-qc/9810044];
- [25] R. J. Gleiser & C. N. Kozameh, “Astrophysical limits on quantum gravity motivated birefringence” Phys. Rev. D **64**, 083007 (2001) [arXiv:gr-qc/0102093].
- [26] Y. Z. Fan, D. M. Wei and D. Xu, arXiv:astro-ph/0702006.
- [27] F. Aharonian *et al.* [The HEGRA Collaboration], Astrophys. J. **614**, 897 (2004) [arXiv:astro-ph/0407118].
- [28] T. Jacobson, S. Liberati and D. Mattingly, Nature **424**, 1019 (2003) [arXiv:astro-ph/0212190].
- [29] R. Montemayor and L. F. Urrutia, Phys. Rev. D **72**, 045018 (2005) [arXiv:hep-ph/0505135];
R. Montemayor and L. F. Urrutia, Phys. Lett. B **606**, 86 (2005) [arXiv:hep-ph/0410143].
- [30] G. Amelino-Camelia, J. Kowalski-Glikman, G. Mandanici and A. Procaccini, Int. J. Mod. Phys. A **20**, 6007 (2005) [arXiv:gr-qc/0312124].
- [31] J. R. Ellis, N. E. Mavromatos and D. V. Nanopoulos, Phys. Rev. D **61**, 027503 (2000) [arXiv:gr-qc/9906029];
Ibid, Phys. Rev. D **62**, 084019 (2000) [arXiv:gr-qc/0006004].

- [32] J. R. Ellis, N. E. Mavromatos and A. S. Sakharov, *Astropart. Phys.* **20**, 669 (2004) [arXiv:astro-ph/0308403].
- [33] Nolan, P. L., et al. 1993, *ApJ*, 409, 697
- [34] J. G. Kirk, Y. Lyubarskyi & J. Pétri (2007) “The theory of pulsar winds and nebulae”, *ArXiv Astrophysics e-print*, astro-ph/0703116,
- [35] A. Achterberg, Y. A. Gallant, J. G. Kirk & A. W. Guthmann (2001) *MNRAS* 328, 393
- [36] M. F. Bietenholz, J. J. Hester, D. A. Frail and N. Bartel, *Astrophys. J.* **615** (2004) 794 [arXiv:astro-ph/0408061].
- [37] Hester, J. J. 1998, *Revista Mexicana de Astronomia y Astrofisica Conference Series*, 7, 90
- [38] K. Mori, D. N. Burrows, J. J. Hester, G. G. Pavlov, S. Shibata and H. Tsunemi, *Astrophys. J.* **609** (2004) 186 [arXiv:astro-ph/0403287].
- [39] F. D. Seward, W. H. Tucker and R. A. Fesen, *Astrophys. J.* **652** (2006) 1277 [arXiv:astro-ph/0608485].
- [40] M. G. F. Kirsch *et al.*, arXiv:astro-ph/0604097.
- [41] C. F. Kennel and F. V. Coroniti, *Astrophys. J.* **283** (1984) 694.
- [42] K. Mori et al (2004) *ApJ* 609, 186
- [43] Clear, J., Bennett, K., Buccheri, R., Grenier, I. A., Hermesen, W., Mayer-Hasselwander, H. A., & Sacco, B. 1987, *A&A*, 174, 85
- [44] de Jager, O. C., & Harding, A. K. 1992, *ApJ*, 396, 161
- [45] Hillas, A. M. et al. 1998, *ApJ*, 503, 744
- [46] J. Kildea *et al.*, *Prepared for 29th International Cosmic Ray Conference (ICRC 2005), Pune, India, 3-11 Aug 2005*
- [47] R. M. Wagner *et al.* [MAGIC Collaboration], *Prepared for 29th International Cosmic Ray Conference (ICRC 2005), Pune, India, 3-11 Aug 2005*
- [48] F. Aharonian *et al.* [H.E.S.S. Collaboration], *Astron. Astrophys.* **457** (2006) 899 [arXiv:astro-ph/0607333].
- [49] C. F. Kennel and F. V. Coroniti, *Astrophys. J.* **283** (1984) 710.
- [50] M. J. Rees and J. E. Gunn, *Mon. Not. Roy. Astron. Soc.* **167** (1974) 1.
- [51] R. T. Emmering & R. Chevalier (1987) *ApJ* 321, 334
- [52] M. C. Begelman & Z. Y. Li (1992) *ApJ* 397, 187
- [53] E. van der Swaluw (2003) *A&A* 404, 939
- [54] Marsden, P. L., Gillett, F. C., Jennings, R. E., Emerson, J. P., de Jong, T., & Olton, F. M. 1984, *ApJL*, 278, L29
- [55] J. G. Kirk (2005) “Particle Acceleration in Relativistic Flows” arXiv:astro-ph/0503316
- [56] G. Morlino, P. Blasi & M. Vietri (2007) *ApJ* 658, 1069
- [57] J. G. Kirk, A. W. Guthmann, Y. A. Gallant, A. Achterberg (2000) *ApJ* 542, 235
- [58] Atayan, A. M., & Aharonian, F. A. 1996, *MNRAS*, 278, 525; F. A. Aharonian and A. M. Atayan, arXiv:astro-ph/9803091.
- [59] Landau, L. D., & Lifchitz, E., “Physique théorique”, tome IV, éditions MIR (1973)
- [60] R. Lieu and W. I. Axford, *Astrophys. J.* **416** (1993) 700.
- [61] W.-M. Yao W M *et al.* [The Particle Data Group] 2006 *J. Phys.* **G 33** 1
- [62] Bevington, P. R. & Keith Robinson, D., “Data reduction and error analysis for the physical sciences”, WCB/McGraw-Hill, Second edition (1992)